

Protograph LDPC Code Design for Asynchronous Random Access

Federico Clazzer, Balázs Matuz, Sachini Jayasooriya, Mahyar Shirvanimoghaddam
and Sarah J. Johnson

Abstract

This work addresses the physical layer channel code design for an uncoordinated, frame- and slot-asynchronous random access protocol. Starting from the observation that collisions between two users yield very specific interference patterns, we define a surrogate channel model and propose different protograph low-density parity-check code designs. The proposed codes are both tested in a setup where the physical layer is abstracted, as well as on a more realistic channel model, where finite-length physical layer simulations of the entire asynchronous random access scheme, including decoding are carried out. We find that the abstracted physical layer model overestimates the performance when short blocks are considered. Additionally, the optimized codes show gains in supported channel traffic – a measure of the number of terminals that can be concurrently accommodated on the channel – of around 17% at a packet loss rate of 10^{-2} w.r.t. off-the-shelf codes.

I. INTRODUCTION

Driven by the emerging machine-to-machine (M2M) communications and the Internet of things services, the number of connected devices is expected to reach the impressive number of 50 billion by 2025 [1]. One of the key challenges – still largely unresolved in the current release of the 5G standard [2] – is the problem on how to efficiently share the medium among a vast population of terminals intermittently and, possibly unpredictably, sending small data

F. Clazzer and B. Matuz are with the Inst. of Communications and Navigation, German Aerospace Center (DLR), Oberpfaffenhofen, Wessling, Germany (e-mail: {federico.clazzer,balazs.matuz}@dlr.de),

S. Jayasooriya and S. J. Johnson are with the School of Electrical Engineering and Computing, The University of Newcastle, University Dr, Callaghan NSW 2308 Newcastle, Australia (e-mail: {sarah.johnson,sachini.jayasooriya}@newcastle.edu.au),

M. Shirvanimoghaddam is with the Faculty of Engineering, The University of Sydney, NSW 2006 Sydney, Australia (e-mail: mahyar.shirvanimoghaddam@sydney.edu.au)

Part of this work has been presented at the IEEE 10th International Symposium on Turbo Codes Iterative Information Processing (ISTC), 2018, Hong Kong.

packets. The change in perspective required by the characteristic of M2M data traffic calls for novel solutions to the medium access problem. The classic scheduled approach, well-suited for the transmission of large amounts of data, becomes rapidly inefficient due to the overhead required to assign resources to users. In particular, exchange of signaling information may become even larger than the data packet itself, and drastically lowers the efficiency of the medium access policy (see for example the physical random access channel (PRACH) procedure [3]).

A natural solution to reduce the signaling overhead, and thus increasing the achievable efficiency is to rely on random access techniques. In recent years, the classic ALOHA and slotted ALOHA (SA) schemes [4], [5] have inspired a flourishing of novel medium access protocols that can be collectively labeled as *modern random access* [6], [7], [8], [9], [10]. In all these schemes, nodes send proactively multiple copies of the same packet, while successive interference cancellation (SIC) enhances the receiver and helps in resolving contention. The pioneer of these schemes is contention resolution diversity slotted ALOHA (CRDSA) [6]¹ where the nodes are enforced to transmit 2 packet copies per transmission attempt [6]. The CRDSA protocol shows a great performance gain compared to SA. Tools borrowed from the theory of codes on graphs [14], [15] enable an asymptotic analysis of the performance [7], when the delay among replica grows very large. The analysis suggests that a variable number of packet copies per user is beneficial. The probability mass function of these packet copies is called *user degree distribution*. Analysis of the finite length performance (when the delay among replicas becomes bounded) have shown that good user degree distributions discovered for the asymptotic setting perform well also in the bounded delay regime [16], [17].

A further extension is proposed in [8], where instead of simply *repeating* the packets prior transmission, a coded version is generated. Such a modification is able to achieve higher energy efficiency, compared to [7]. In [8], also an achievable throughput region for the collision channel is derived. Impressively, letting the maximum number of replicas and delay among them grow large is sufficient to achieve the limit of 1 packet per slot in the collision channel [18]. This remarkable result shows that such schemes are able to close the gap to coordinated and orthogonal medium access schemes. Along a similar line of research, in [10] the authors investigate the behavior of a random access protocol with repetitions where the frame dimension is not set a-priori but it is dynamically adapted for maximizing

¹Concurrently also [11] proposed a random access tree-resolution scheme that relies on the use of SIC at the receiver, which is able to largely outperform the classic standard and modified tree-algorithms [12], [13].

the throughput.

In [19] an information theoretic rate bound that considers the finite length nature of M2M communications and a more realistic channel model is derived. The paper shed the light on the gap between practical schemes like CRDSA and the achievable bound, raising awareness to a larger community about the energy-efficiency problem. A new wave of research has been initiated, bringing several new approaches to the uncoordinated (and unsourced) multiple-access problem, e.g. [20], [21], [22], [23], [24].

The relaxation of slot-synchronicity reduces the complexity and especially power consumption of the transmitter devices. Avoiding the need to keep synchronization to a common clock, enables longer *sleep* times for the nodes. This is of outermost importance in many M2M scenarios, where devices are powered via batteries that cannot (or may not) be replaced for their entire lifetime. Some recent solutions derived from the *asynchronous* ALOHA protocol have shown to be competitive in comparison with their slot-synchronous counterpart [25], [26], [27], [28]. These solutions also adopt the transmission of multiple copies of the packets and SIC at the receiver. When the receiver entangles combining techniques, e.g. maximal-ratio combining, with SIC slot-synchronous protocols may be outperformed [27].²

In this work, we consider an asynchronous random access scheme. We assume that every packet (codeword) is subject to additive white Gaussian noise (AWGN) and possibly to interference. Due to the asynchronous nature of the scheme the interference may affect different portions of the packet with different power, depending on the number of colliding users. In order to allow reliable transmission on the asynchronous random access channel, a suitable error protection scheme needs to be used. Works in the literature usually assume capacity achieving random code ensembles and apply a threshold based model for decoding [25]: the average signal to noise plus interference ratio over a packet is compared to the Shannon limit, i.e., the worst channel parameter for which error free transmission is possible, to decide whether decoding is possible or not. In [29], the authors replace the Shannon limit by iterative decoding thresholds of some off-the-shelf low-density parity-check (LDPC) code ensembles. In an earlier conference paper [30], we considered a decoding region (which can be seen as a multi-dimensional threshold based model) to perform dedicated protograph-based LDPC code design for the asynchronous random access channel and to estimate the packet loss rate (PLR) of the random access protocol. However, it remains an open question how

²The performance heavily depends on the specific configuration, i.e. number of replicas, physical layer forward error correction, channel conditions, etc.

accurately such threshold based models can predict the PLR.

The code design of [30] using a multi-dimensional threshold based model can be seen as a type of code design for unequal error protection. Unequal error protection using error correcting codes has long been studied in the literature for different channels. Early works date back to the 1960s. For instance, [31] addresses the problem of achieving different bit error probabilities in different parts of the decoded codeword. More recently, both turbo codes and LDPC codes have been designed for channels that introduce different reliabilities on different parts of the codeword [32], [33], [34] to counteract the effect of block fading: a block is characterized by a constant fading coefficient, while block by block the fading coefficient is independently drawn from a predefined distribution.

In the following, we focus on the asynchronous random access channel for which we provide tailored protograph LDPC code designs. Here, we make use of a surrogate channel model to simplify the code design. We show that the resulting codes evidently boost the medium access (MAC) performance, even in comparison with the most competitive code designs for standard AWGN channels. As an extension of [30], we do not restrict to finding LDPC code ensembles with favorable iterative decoding thresholds only, but also design finite-length codes. These codes are used to simulate the physical layer of the random access protocol, giving a more realistic estimate of the PLR. The key contributions of the paper can be summarized as follows:

- In Section III we present a surrogate channel model, exploited in the code design phase, which assumes constant interference power over a fraction α of the codeword. To facilitate code design, we further approximate the aggregate interference contribution, possibly generated by a multitude of terminals, as Gaussian. In Section III-D, we present a protograph LDPC code design for this channel model and its iterative decoding threshold is compared with the one of a raptor-like LDPC code design proposed for the recently introduced fifth generation of mobile networks (5G) standard. Both code designs are compared with the Shannon limit.
- The impact of the Gaussian interference assumption on the code performance is also considered in Section III-E. The expression of the log-likelihood ratio (LLR) and the threshold performance, computed with quantized density evolution, are presented for a single interferer when the Gaussian assumption is dropped.
- In order to get a first – yet not fully accurate – performance characteristic for the proposed LDPC codes in the random access (RA) channel, we elaborate on the decoding condition so as to abstract the physical layer in Section IV-A. A decoding region, as a function

of the interference pattern for both a random code ensemble and for the LDPC code ensemble is derived. Although more accurate than the surrogate channel model, since the effective interference power and affected codeword position is considered, the abstraction grounds on the iterative decoding threshold, and thus on large blocks assumption.

- Since RA is particularly appealing for short packet transmission, we depart from the physical layer abstraction, and present in Section IV-B physical layer simulations considering finite block length. Interestingly, the codes designed for the surrogate channel model still perform very well on the asynchronous multiple access channel. Moreover, the performance trends and relative performance identified via the simpler simulations with the abstracted physical layer are confirmed.

II. SYSTEM MODEL

In this Section we describe the system model, starting with the medium access policy in II-A. Section II-B follows with the physical layer model.

A. Asynchronous Random Access Protocol

We consider an uncoordinated asynchronous random access protocol based on [25], [26].³ An infinite user population generates data traffic modeled as a Poisson process with intensity G , called the *channel load*. It is measured in packet arrivals per packet duration t_p . Specifically, the probability distribution that u users initiate a transmission within a packet duration is $P(u) = \frac{G^u e^{-G}}{u!}$.

Users are allowed to make a single attempt to transmit their data, i.e., no re-transmissions are considered. Prior to transmission, the data packet is replicated $d = 2$ times. We refer to each copy as a *replica*. The replicas are transmitted adhering the following rules:

- 1) self-interference must be avoided, i.e. no portion of the two replicas shall overlap;
- 2) the maximum delay – called virtual frame (VF) – between the start of the first replica and the end of the second one shall not exceed t_f seconds;
- 3) the delay between the start of the two replicas is drawn uniformly at random within the interval $\left(t_0^{(u)} + t_p, t_0^{(u)} + t_f - t_p\right]$, with $t_0^{(u)}$ the activation time of user u .

Once the transmission times for the replicas are chosen, this information is stored in the header in order to enable SIC at the receiver. Then the replicas are encoded so to be protected against noise and multiple access interference.

³With respect to [25], no concept of MAC frame is present, so that the terminals operate in a full asynchronous scenario. Compared to [26], local time slots constraining the transmission delay between replicas of the same user are eliminated.

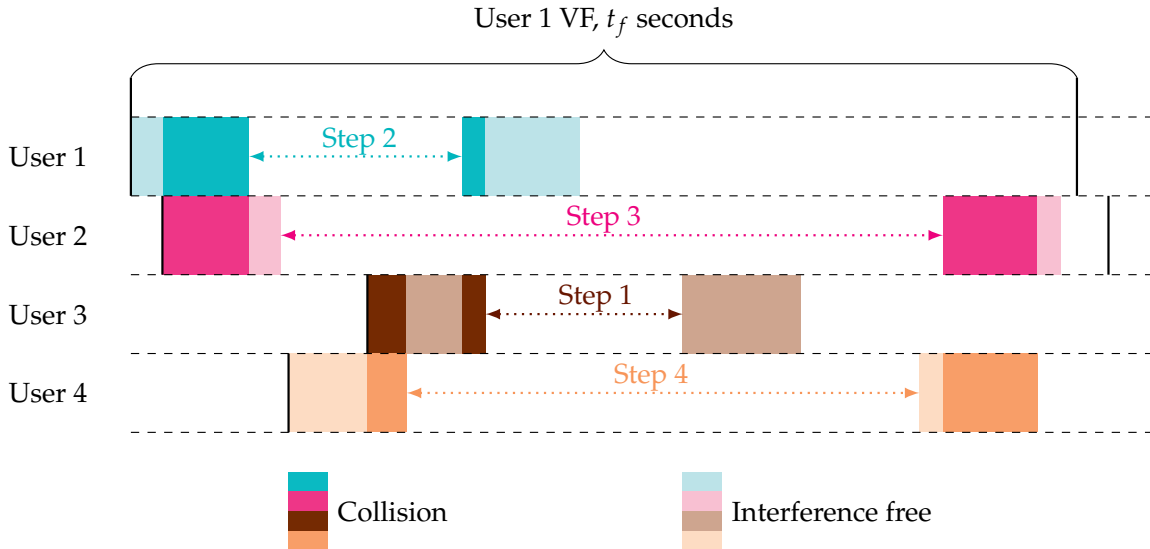


Fig. 1: Example of collision pattern at the receiver, and of the SIC procedure. Upon correct decoding, SIC removes the packet and its twin.

At the receiver side, the incoming signal is sampled, stored and subsequently processed. The receiver makes use of a decoding window of size W samples. At first, replicas are detected, e.g., with correlation-based rules [35], [36].⁴ Channel estimation is performed (for details see Section II-B). The soft-demodulator provides bit-wise LLRs as input to the channel decoder. When the cyclic redundancy check (CRC) matches, the replica is declared as correctly decoded. When this is the case, readily two operations follow:

- 1) the replica waveform is reconstructed on a sample level and subtracted from the incoming signal;⁵
- 2) the information about the twin location (the time position of the other replica of the same user) is extracted from the header.

The second operation is followed by data-aided channel estimation on the packet copy. In fact, the entire data carried by the packet is now known and can be used as pilots for refining channel estimation. The received waveform of the twin can be reconstructed and removed from the received signal. We shall note that if a replica can be decoded, the interference reduction triggered by SIC may impact underlying collided packets and can lead to further

⁴In this work ideal detection is considered, i.e., all transmitted replicas can be detected by the receiver and no false alarms are present.

⁵We will consider ideal interference cancellation, i.e. after cancellation no residual power is left by the replica.

packet recovery. The receiver proceeds extracting the second candidate replica and repeats the aforementioned operations. SIC is iterated until no more packets are present in the decoding window, or when a predefined maximum number of iterations is reached. The second option is normally adopted when the receiver has tighter complexity or delay constraints. Once the operations on the current receiver decoding window are terminated, the receiver window is shifted forward by $\Delta W \ll W$ samples, and the detection of the replicas is initiated again.

Example 1: Consider an instance of SIC as depicted in Figure 1. A SIC step consists of successfully decoding a replica and removing it as well as its twin from the received signal. Thus, in Figure 1, the first SIC step consists of decoding the second replica of user 3, since it is interference free. Then, the contribution of both replicas can be removed from the received signal. Consequently, the second replica of user 1 and the first replica of user 4 become interference-free. We decode user 1, remove both replicas from the signal. We proceed in the same way for user 2. Since no interference is present anymore, we assume that also the user 4 can be successfully decoded.

Note that replicas with the lowest level of interference are the ones with the highest chance to be correctly decoded. Interference-free replicas or replicas collided with a single interferer have the highest chance to be recovered in a SIC iteration. Considering the latter, collision of *two* packets yields interference which is either at the beginning or at the end of a packet. Consequently, an error-correcting code able to better protect the beginning or the end of a packet, should come to the aid of SIC improving the random access overall performance. In light of this, in Section III we focus on the design of error correcting codes able to better protect the beginning and end of a codeword.

B. Asynchronous Random Access Channel Model

In the following, we define the general channel model for the considered random access scheme. Assume that all replicas of all users form the set \mathcal{R} . Consider the r -th replica in \mathcal{R} . The transmitted signal $x^{(r)}$ corresponding to the modulated codeword $\mathbf{a}^{(r)} = (a_0^{(r)}, a_1^{(r)}, \dots, a_{n_s-1}^{(r)})$ is

$$x^{(r)}(t) = \sum_{i=0}^{n_s-1} a_i^{(r)} g(t - it_s)$$

where n_s is the number of modulation symbols in a packet, t_s is the symbol duration, and $g(t)$ is the pulse shape. The received signal is in general affected by a frequency offset, modeled as a uniformly distributed random variable $f^{(r)} \sim \mathcal{U}[-f_m; f_m]$, with f_m the maximum frequency

offset. A sampling epoch, also modeled as a uniformly distributed random variable $\epsilon^{(r)} \sim \mathcal{U}[0; t_s]$ [37, Ch. 2]. Both frequency offset and sampling epoch are common to each replica of the same user, but independent user by user. Furthermore, the signal is also affected by phase offset $\varphi^{(r)}$, modeled as a uniformly distributed random variable between 0 and 2π , i.e., $\varphi^{(r)} \sim \mathcal{U}[0; 2\pi)$. The phase offset is assumed to be independent replica by replica. Further, we assume AWGN. No fading is considered which is typical, e.g., for fixed-terminal geostationary orbit satellite scenarios. For $f_m t_s \ll 1$, the received signal $y(t)$ after matched filtering, which is a superposition of all replicas $r \in \mathcal{R}$, is

$$y(t) = \sum_{r \in \mathcal{R}} \tilde{x}^{(r)}(t - \epsilon^{(r)} - t_0^{(r)}) e^{j(2\pi f^{(r)} + \varphi^{(r)})} + n(t) \quad (1)$$

where $\tilde{x}^{(r)}(t)$ is the matched filtered signal $x^{(r)}(t)$. In equation (1), $t_0^{(r)}$ is the r -th replica delay w.r.t. the common reference time. The noise term $n(t)$ is given by $n(t) \triangleq \nu(t) * g(t)$, where $\nu(t)$ is a white Gaussian process with single-sided power spectral density N_0 . For the sake of simplicity, throughout the paper we make the assumptions that $f^{(r)} = 0$ and $\epsilon^{(r)} = 0$, $\forall r \in \mathcal{R}$. Hence, equation (1) becomes

$$y(t) = \sum_{r \in \mathcal{R}} \tilde{x}^{(r)}(t - t_0^{(r)}) e^{j\varphi^{(r)}} + n(t).$$

We focus again on replica r . After ideal detection, the received signal corresponding to r can be identified and isolated. Ideal channel estimation recovers perfectly the phase offset $\varphi^{(r)}$. After compensation, the discrete-time version of the received signal $\mathbf{y}^{(r)} = (y_0^{(r)}, \dots, y_{n_s-1}^{(r)})$ corresponding to the replica r is given by

$$\mathbf{y}^{(r)} = \mathbf{a}^{(r)} + \mathbf{z}^{(r)} + \mathbf{n}^{(r)}. \quad (2)$$

Here $\mathbf{n}^{(r)} = (n_0^{(r)}, \dots, n_{n_s-1}^{(r)})$ are the samples of a complex discrete white Gaussian process with $n_i^{(r)} \sim \mathcal{CN}(0, 2\sigma_n^2)$, $\forall i \in \{0, \dots, n_s - 1\}$, $\forall r \in \mathcal{R}$. The aggregate interference contribution over the replica- r signal is $\mathbf{z}^{(r)} = (z_0^{(r)}, \dots, z_{n_s-1}^{(r)})$, with

$$z_i^{(r)} = \sum_{\bar{r} \in \mathcal{R} \setminus r} \tilde{x}^{(\bar{r})}(kt_s - \Delta t_0^{(\bar{r})}) e^{j\Delta\varphi^{(\bar{r})}} \quad \text{for all } i \in \{0, \dots, n_s - 1\}.$$

Here, $\Delta t_0^{(\bar{r})} = t_0^{(r)} - t_0^{(\bar{r})}$ and $\Delta\varphi^{(\bar{r})} = \varphi^{(r)} - \varphi^{(\bar{r})}$. The instantaneous received power for symbol i is $P_i^{(r)} \triangleq \mathbb{E}[|a_i^{(r)}|^2]$. The useful received power is assumed to be constant over the entire replica r , i.e. $P_i^{(r)} = P^{(r)}$ for $i = 0, \dots, n_s$ and for $\forall r \in \mathcal{R}$. Users are received with the same power thanks to perfect power control, i.e. $P^{(r)} = P$ for $\forall r \in \mathcal{R}$. As a result $P_i^{(r)} = P$. The aggregate interference power for symbol i is $Z_i^{(r)} \triangleq \mathbb{E}[|z_i^{(r)}|^2]$. Finally, the

noise power is $2\sigma_n^2$ and we define the signal-to-noise ratio, $E_s/N_0 = P/2\sigma_n^2$. We also define the signal-to-interference ratio $\gamma_i = P/Z_i$.

III. CODE DESIGN FOR THE ASYNCHRONOUS RANDOM ACCESS CHANNEL

A. Protograph LDPC Codes

We propose protograph-based binary LDPC code designs tailored to the interference that occurs in an asynchronous RA scenario. The parity-check matrix of these codes is derived from a relatively small matrix, called a base matrix \mathbf{B} , which represents the code constraints. Alternatively, we may describe the base matrix as a bipartite graph, termed protograph, with n_b variable nodes (VNs) and m_b check nodes (CNs). Non-zero entries $b_{i,j}$ in \mathbf{B} represent connections between VNs of type j and CNs of type i . In order to improve the code performance, we may decide to puncture some of the VN types in the base matrix whose number is denoted by p_b . The number of not punctured variable nodes is denoted by $(n_b - p_b)$. The parity check-matrix of a protograph based (n, k) LDPC code is obtained by expansion or lifting of the base matrix. This is done by copying the protograph $n/(n_b - p_b)$ times and interconnecting the copies among each other following certain rules (see [38] for details). In this work, we consider standard Gray labelled quadrature amplitude shift keying (QPSK) modulation where the binary labels of a symbol consist of two bits. Thus a packet with n_s symbols is protected by an LDPC code with codeword length $n = 2n_s$ bits.

B. Code Optimization

Good base matrices are found by some optimization algorithm, such as differential evolution [39]. The goal is to find protographs which maximize a gain function. To this end, differential evolution creates a generation of candidate base matrices for which the gain function is evaluated. By introducing perturbations on the base matrix entries, a new generation of base matrices is obtained. They may replace the original ones if their gain function is higher. After a certain number of generations we choose those base matrices which maximize the gain function.

The gain function is usually a function of the protograph ensemble's iterative decoding threshold which can be seen as the worst channel parameter for which symbol error probability vanishes (assuming that the block length and the number of decoding iterations go to infinity). We will give a more precise description in the following.

Iterative decoding thresholds can be found using (quantized) density evolution [15], or a suitable approximation, such as extrinsic information transfer (EXIT) analysis [40] if

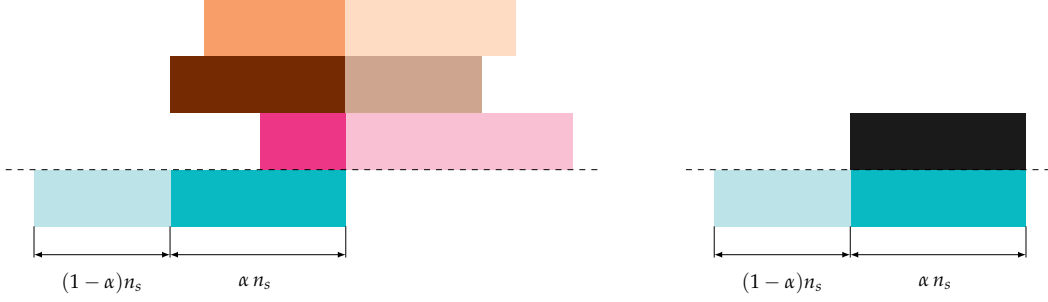


Fig. 2: Collision of multiple users (left) and abstracted surrogate model with constant interference power over αn_s symbols (right).

certain Gaussian assumptions can be made. EXIT analysis simplifies the computation of the protograph code ensemble's compared to (quantized) differential evolution. To compute iterative decoding thresholds, we make use of the channel LLRs distributions for each codeword bit. In the following sections, we discuss the effect of the interference model on the channel LLR distributions and thus on the code design.

C. Simplified Channel Models for Code Design

To facilitate the code design, we assume the following *surrogate* channel model:

- A fraction $1 - \alpha$, $0 \leq \alpha \leq 1$, of a (modulated) codeword is only affected by noise with power $2\sigma_n^2$.
- A fraction α of a (modulated) codeword is affected by noise and interference of constant power over the fraction.

Thus, we make the assumption of a *block interference channel* [41] which is a widely used model in the literature (see, e.g., [27] and references therein). Clearly, this is a simplification, since a codeword in reality may experience various interference levels due to multiple packet collisions. Note also that for our asynchronous RA protocol, the interference is confined to the beginning, the end, or to the beginning and the end of a codeword. This observation is exploited for the code design. The surrogate channel model is exemplified in Figure 2. We will illustrate its validity Section IV.

1) *Gaussian Interference Model*: Consider the interference vector $\mathbf{z}^{(r)}$ in (2). Let its i -th element $z_i^{(r)}$ be non-zero, i.e., the i -th packet symbol is subject to interference. Then, $z_i^{(r)}$ is a sample of a complex Gaussian distribution $\mathcal{CN}(0, 2\sigma_l^2)$, where $2\sigma_l^2$ is the interference power. This assumption is accurate already in case of a few interferers having different phase,

frequency and time offset. When only one interferer affects a packet, the assumption becomes inaccurate. Nevertheless, we will illustrate that it is a reasonable model for the LDPC code design.

Under the assumption of Gaussian interference, the interference plus noise also follows a complex Gaussian distribution $\mathcal{CN}(0, 2\sigma^2)$, with

$$\sigma^2 = \sigma_n^2 + \sigma_i^2.$$

Let us define as $C(\sigma^2)$ the QPSK constraint AWGN channel capacity for a given σ^2 . The corresponding outage capacity C_o for our surrogate channel model in Section III-C under the Gaussian interference assumption becomes

$$C_o(\alpha, \sigma_n^2, \sigma^2) = (1 - \alpha) C\left(\frac{1}{2\sigma_n^2}\right) + \alpha C\left(\frac{1}{2\sigma^2}\right). \quad (3)$$

For a fixed α and σ_n^2 we can invert (3) and write σ^2 (or likewise σ_i^2) as a function of C_o . Then, for a fixed rate, error free transmission is possible if the interference power $\sigma_i^2 < \sigma_{i,o}^2$, where $\sigma_{i,o}^2$ is referred to as the Shannon limit.

Code design for the case of the Gaussian interference model becomes equivalent to code design for an AWGN channel where codeword bits are subjected to one of two possible noise levels. The design of LDPC photograph codes for this channel is well studied and, given the interference is modeled as Gaussian noise, various approximations to density evolution, such as EXIT charts, are well verified in this scenario.

2) *Single Interferer Model*: The Gaussian interference model is a reasonable approximation already in presence of a few interferers under the assumption of time, frequency and phase offset. When a single interferer is present over the codeword, the Gaussian model may become imprecise and the interference shall be better characterized, taking into account the chosen modulation. Thus in this Section, we consider a codeword affected by interference generated by a single QPSK-modulated interferer, received with the same power. After ideal detection and ideal channel estimation, the interference occurring on a codeword symbol i presents a relative phase shift $\Delta\varphi^{(1)}$, and a relative epoch $0 < \Delta\epsilon^{(1)} < t_s$. Hence, the interference on codeword symbol i , i.e. z_i , can be expressed as

$$z_i = \tilde{x}^{(1)}(kt_s - \Delta\epsilon^{(1)} - \Delta t_0^{(1)})e^{j\Delta\varphi^{(1)}}.$$

Note that $\gamma_i = P/Z_i = 1$. For ease of notation we drop the superscript (1) , so that $\Delta\varphi^{(1)} \triangleq \Delta\varphi$ and $\Delta\epsilon^{(1)} \triangleq \Delta\epsilon$. Figure 3 shows the considered scenario. The i -th codeword symbol is

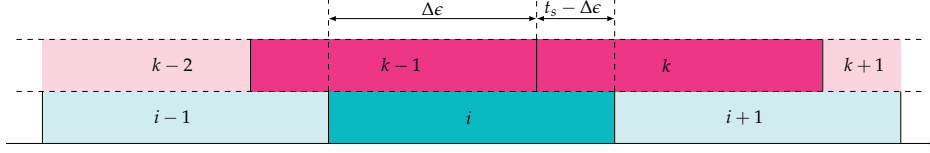


Fig. 3: The i -th codeword symbol (azure) affected by a single interferer (red), with a relative epoch of $\Delta\epsilon$. Both interferer symbol $k - 1$ and k impact the codeword symbol i .

interfered by a portion $\Delta\epsilon$ of symbol duration with the $(k - 1)$ -th symbol of the interferer and by $t_s - \Delta\epsilon$ with the k -th symbol of the interferer. We define $\mathcal{S} = \{S_1, S_2, S_3, S_4\}$ as the set of QPSK constellation points with respective labels $\{00, 01, 11, 10\}$. For a given relative epoch $\Delta\epsilon$, and a relative phase offset $\Delta\varphi$, known at the receiver, the channel LLR of bit level 1 of a Gray labeled QPSK signal are given by

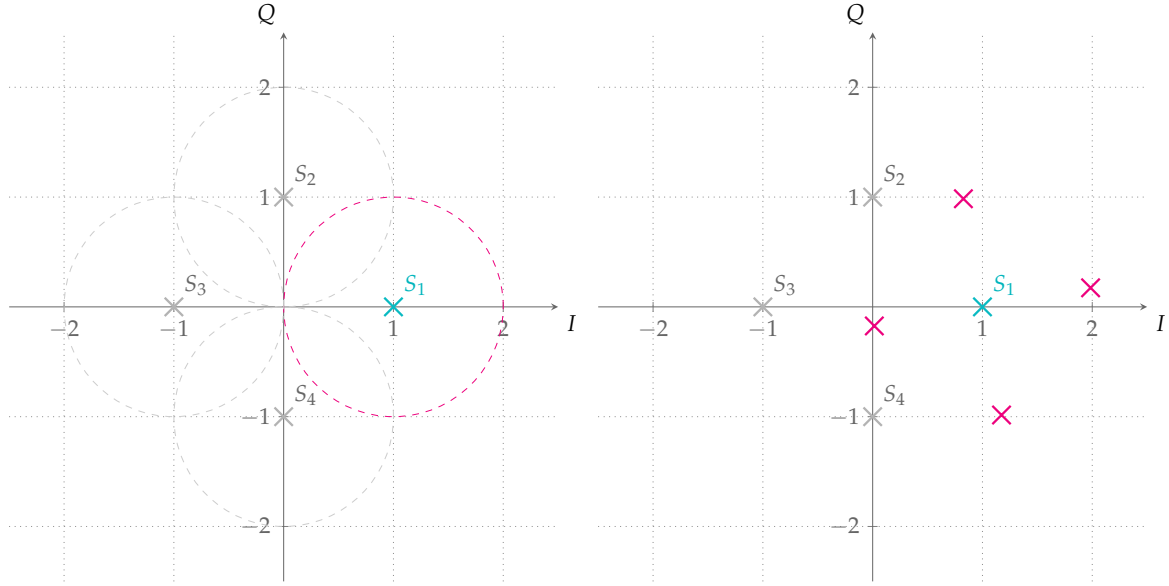
$$L_1(y, \Delta\varphi, \Delta\epsilon') = \log \left[\frac{\sum_{\{S_{k-1}, S_k\} \in \mathcal{S}^2} \left(e^{-\frac{|y - S_1 - e^{j\Delta\varphi}(\Delta\epsilon' S_{k-1} + (1 - \Delta\epsilon') S_k)|^2}{2\sigma_n^2}} + e^{-\frac{|y - S_2 - e^{j\Delta\varphi}(\Delta\epsilon' S_{k-1} + (1 - \Delta\epsilon') S_k)|^2}{2\sigma_n^2}} \right)}{\sum_{\{S_{k-1}, S_k\} \in \mathcal{S}^2} \left(e^{-\frac{|y - S_3 - e^{j\Delta\varphi}(\Delta\epsilon' S_{k-1} + (1 - \Delta\epsilon') S_k)|^2}{2\sigma_n^2}} + e^{-\frac{|y - S_4 - e^{j\Delta\varphi}(\Delta\epsilon' S_{k-1} + (1 - \Delta\epsilon') S_k)|^2}{2\sigma_n^2}} \right)} \right] \quad (4)$$

Where we defined $\Delta\epsilon' \triangleq \Delta\epsilon/t_s$. For the sake of simplification, we assume symbol-synchronous interference i.e. $\Delta\epsilon = \Delta\epsilon' = 0$ and unknown, uniformly distributed relative phase offset. We can write the the channel LLR of bit level 1 as:

$$L_1(y, \Delta\epsilon = 0) = \log \left[\frac{\sum_{S_k \in \mathcal{S}} \int_{-\pi}^{\pi} \left(e^{-\frac{|y - S_1 - S_k e^{j\Delta\varphi}|^2}{2\sigma_n^2}} + e^{-\frac{|y - S_2 - S_k e^{j\Delta\varphi}|^2}{2\sigma_n^2}} \right) d\theta}{\sum_{S_k \in \mathcal{S}} \int_{-\pi}^{\pi} \left(e^{-\frac{|y - S_3 - S_k e^{j\Delta\varphi}|^2}{2\sigma_n^2}} + e^{-\frac{|y - S_4 - S_k e^{j\Delta\varphi}|^2}{2\sigma_n^2}} \right) d\theta} \right]. \quad (5)$$

Figure 4 shows the possible received symbol i after phase compensation with no noise when symbol S_1 (or S_2, S_3, S_4) is transmitted. The received symbol can lay anywhere on the red circle if no assumption on interference relative phase shift is done, see Figure 4a. If a relative shift of $\Delta\varphi = 10^\circ$ is present, then any of the four red points can be received depending on the transmitted interference symbol k , see Figure 4b.

In Figure 5 the probability density function (PDF) of the bit LLRs assuming a symbol-synchronous QPSK interferer with either uniform at random phase or with a fixed relative



(a) QPSK modulated constellation after phase compensation at the receiver side. We highlight symbol $S_1 = (1, 0)$. If the symbol is affected by QPSK modulated interference with the same unit power, no noise, and random phase the received symbol will lay on the red unit circle centered in $(1, 0)$.

(b) QPSK modulated constellation after phase compensation at the receiver side and one QPSK modulated interferer with the same unit power, no noise, and $\Delta\varphi = 10^\circ$ relative phase shift. Red crosses represent the four possible received symbols if the considered transmitted symbol was $S_1 = (1, 0)$.

Fig. 4: QPSK modulated constellation after phase compensation at the receiver side and single symbol-synchronous interferer with same power, relative phase shift and no noise.

phase offset plus AWGN noise with $E_s/N_0 = 6$ dB is shown. For the plot we assume that either symbol S_0 or S_1 has been transmitted, i.e., bit level one is zero. The curve with $\Delta\varphi = 0$ shows the PDF of the bit LLRs for the case of aligned phase. The channel LLRs are no-longer Gaussian and thus quantized density evolution, which passes the entire LLR though the decoding algorithm, rather than a Gaussian model, will be used to calculate the code thresholds.

D. Code Design for Gaussian Interference

Two different code designs for the surrogate channel with Gaussian interference, as defined in Section III-C1, are presented next. The designs are exemplified for a code rate of $R_c = 1/2$, QPSK modulation and a target $E_s/N_0 = 6$ dB, typical parameters for an asynchronous RA

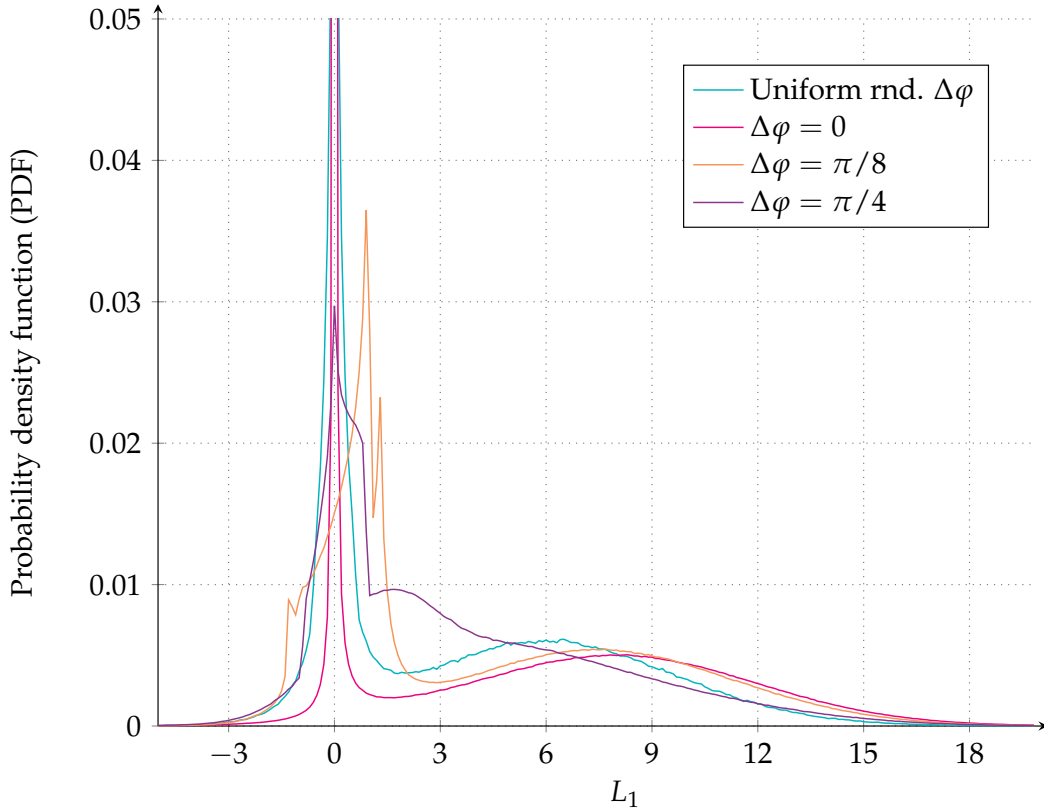


Fig. 5: Probability density function of the bit LLRs assuming AWGN and symbol-synchronous QPSK interferer with uniform at random phase (or with a fixed phase offset) when $E_s/N_0 = 6$ dB.

scheme [25], [26]. However, the code design can be easily performed for any other parameter set.

1) *Ad-hoc LDPC Code Design:* Observe that the interference present in the random access channel may affect the beginning, the end, and sometimes both beginning and end of a packet. In fact, by analyzing the interference patterns, we found that the third case, where the interference affects both the beginning and end of a packet, is a case of limited interest for the code design (although it is not difficult to embed additional constraints in the code design). To see this, consider the collision of two packets. Clearly, the interference here hits the beginning or end of a packet. Consider now that three packets collide such that there exists a packet with interference both at the beginning and at the end. Then, the two remaining packets will experience a lower level of interference which is either at the beginning or at the end. So SIC may preferably decode one of those packets, and cancel their contribution from the received signal. Similar considerations can be made when four packets collide and

we have a packet with both interference at the beginning and the end. For five or more interfering packets there could conceivably be cases where a packet with interference at both the beginning and end might be favorable to decode first, but for the code design we focus on the most frequent cases. Thus, we tailor our code design to these specific interference patterns by targeting codes which are robust w.r.t. interference at the beginning or at the end of a codeword.

In the following, we target code designs robust to interference at the beginning or end of a codeword by imposing certain symmetry constraints on the code's base matrix \mathbf{B}_A . Let us split $\mathbf{B}_A = [\mathbf{B}_P | \mathbf{B}_{T_x}]$ into two submatrices, an $m_b \times p_b$ matrix \mathbf{B}_P for the punctured columns and an $m_b \times (n_b - p_b)$ matrix \mathbf{B}_{T_x} composed by all columns which are not punctured. For the entries $b_{i,j}$ of \mathbf{B}_{T_x} we impose

$$b_{(m_b-i-1), (n_b-p_b-j-1)} \stackrel{!}{=} b_{i,j} \quad (6)$$

$\forall i \in \{0, \dots, m_b - 1\}$ and $\forall j \in \{0, \dots, n_b - p_b - 1\}$. The symmetry requirement in (6) states that the j -th column of \mathbf{B}_{T_x} from the left shall be equal to the j -th column from the right, whose elements are however placed in a reversed order. A similar requirement is put on the submatrix \mathbf{B}_P .

For the protograph search by means of differential evolution we fix n_b , m_b , and p_b , such that the code rate $R_c = \frac{n_b - m_b}{n_b - p_b}$. We also fix σ_n^2 (e.g., as a result of link budget considerations) and look for protographs which for certain α , allow successful decoding at an interference power $2\sigma_t^2$ as high as possible. Thus, the iterative decoding threshold is the maximum interference power for a certain α and σ_n^2 , such that the probability of symbol error in a codeword vanishes. Since α is the outcome of random process, we are interested in a code design that is robust for various values of α , denoted by $\alpha^{(\ell)}$. This implies a multi-target optimization. Due to complexity reasons, we resort to only a few different $\alpha^{(\ell)}$ for which we simultaneously optimize our base matrices.

The Gaussian interference model yields channel LLRs for the two QPSK bit-levels which are Gaussian distributed. For this setup, EXIT analysis [40] is known to provide accurate iterative decoding threshold estimates. Thus, for each $\alpha^{(\ell)}$ we aim at determining the maximum amount of interference $\sigma_{t,\text{th}}^2(\alpha^{(\ell)})$, such that error-free decoding is possible. Following the results in [40], this requires that the log-likelihood a posteriori probability (APP) mutual information $I_{\text{APP}}(j) \rightarrow 1 \forall j \in \{0, \dots, n_b - 1\}$ (assuming that the block length and the number of decoding iterations go to infinity).

For a general code ensemble, the computation of the iterative decoding threshold has to take into account the respective cases of the interferer being at the beginning or end of the codeword. Let us denote by $\sigma_{i,\text{th}}^2(\alpha^{(\ell)}, \text{b})$ and by $\sigma_{i,\text{th}}^2(\alpha^{(\ell)}, \text{e})$ the iterative decoding threshold for a chosen $\alpha^{(\ell)}$, when the interferer affects the beginning or end of the codeword, respectively. We evaluate the following gain function g ,

$$g = \prod_{\ell} \frac{\sigma_{i,\text{th}}^2(\alpha^{(\ell)}, \text{b})}{\sigma_{i,\text{o}}^2(\alpha^{(\ell)})} \cdot \frac{\sigma_{i,\text{th}}^2(\alpha^{(\ell)}, \text{e})}{\sigma_{i,\text{o}}^2(\alpha^{(\ell)})}, \quad (7)$$

where $\sigma_{i,\text{o}}^2$ is obtained from the outage capacity expression in (3). Note that due to the symmetry constraint in (6), $\sigma_{i,\text{th}}^2(\alpha^{(\ell)}, \text{b}) = \sigma_{i,\text{th}}^2(\alpha^{(\ell)}, \text{e})$ and (7) can be simplified.

Example 2: Fix $n_b = 11$, $m_b = 6$, $p_b = 1$, $R_c = 1/2$, where the first column is punctured. For the multi-target optimization we impose the symmetry constraint in (6). For complexity reasons, we optimize the threshold for only two different values of α , namely $\alpha^{(0)} = 6/10$ and $\alpha^{(1)} = 9/10$. The multi-target optimization yields⁶

$$\mathbf{B}_A = \begin{bmatrix} 1 & 0 & 0 & 2 & 2 & 0 & 0 & 0 & 0 & 1 & 1 \\ 2 & 0 & 0 & 0 & 0 & 0 & 1 & 0 & 1 & 1 & 0 \\ 2 & 0 & 1 & 0 & 1 & 0 & 0 & 0 & 0 & 0 & 1 \\ 2 & 1 & 0 & 0 & 0 & 0 & 0 & 1 & 0 & 1 & 0 \\ 2 & 0 & 1 & 1 & 0 & 1 & 0 & 0 & 0 & 0 & 0 \\ 1 & 1 & 1 & 0 & 0 & 0 & 0 & 2 & 2 & 0 & 0 \end{bmatrix}.$$

2) *Raptor-like LDPC Code Design:* Protograph-based Raptor-like LDPC codes [42] and belong to the class of rate-compatible LDPC codes. The base matrix has the following structure

$$\mathbf{B} = \begin{bmatrix} \mathbf{B}_{\text{pre}} & \mathbf{0} \\ \mathbf{B}_{\text{LT}} & \mathbf{I} \end{bmatrix}$$

where in analogy to Raptor codes \mathbf{B}_{pre} and \mathbf{B}_{LT} represent the base matrix of the precode and Luby transform (LT) code respectively. Further, \mathbf{I} is an identity matrix. Owing to their excellent performance, protograph-based Raptor-like LDPC codes are adapted in the context of the 5G standardization for enhanced mobile broadband (eMBB). During the standardization several proposals for base matrices have been made with very similar performance. We consider one of these 5G proposals for short blocks [43]

⁶The differential evolution algorithm in [39] was executed with the following parameters: crossover probability of 0.6, population size of 200, and number of generations of 4000.

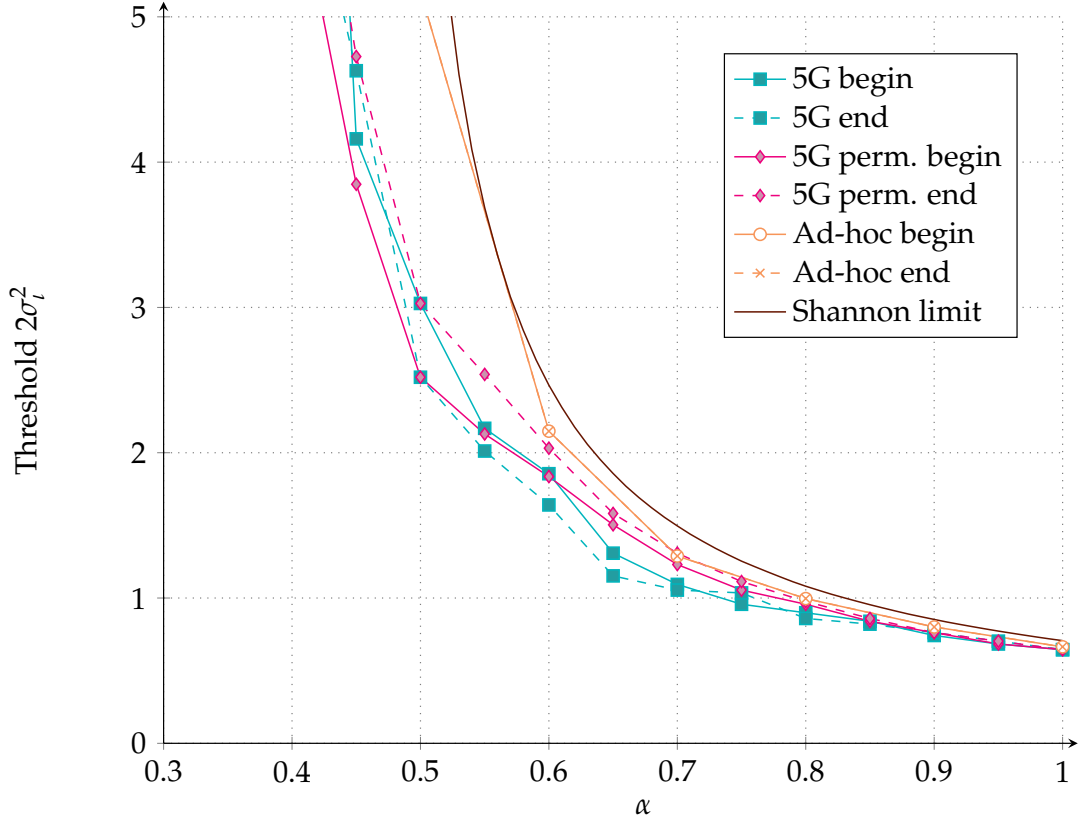


Fig. 6: Maximum interference power versus α for different protographs and outage capacity on a QPSK channel with fixed AWGN at $E_s/N_0 = 6$ dB. The 5G corresponds to the ensemble with base matrix \mathbf{B}_{5G} . The 5G perm. corresponds to the ensemble with base matrix \mathbf{B}_{5G}^π . Ad-hoc corresponds to the ensemble with base matrix \mathbf{B}_A . Begin and end represent the iterative decoding threshold with the interference hitting the codeword from the left or the right respectively.

Observe from the figure that the ad-hoc code design (base matrix \mathbf{B}_A) performs close to the capacity curve. Also, owing to the symmetry constraint in (6), the code ensemble shows a the same behavior for the interference being at the beginning or at the end of a codeword. The 5G-like protograph code ensemble (base matrix \mathbf{B}_{5G}) performs differently if the interferer is from the left or right. By permuting the code (base matrix \mathbf{B}_{5G}^π) as described in Section III-D2 the code ensemble performance gets closer to capacity. Further, for α close to one, both 5G-like and ad-hoc code design perform similarly. This is because here the channel is like a conventional AWGN channel for which 5G codes are known to be among the best LDPC codes.

E. Asymptotic Results for a Single Non-Gaussian Interferer

Although our ad-hoc protograph ensemble was designed for the Gaussian interference model, we show here that its asymptotic performance is also good in this case of non-Gaussian interferers. We consider iterative decoding threshold of our ad-hoc protograph ensemble for two cases:

- Symbol-synchronous, phase-aligned, equal-power QPSK interferer, i.e. $\Delta\epsilon = 0$, $\Delta\varphi = 0$, $P = Z = 1$.
- Symbol-synchronous, equal-power QPSK interferer with uniform at random phase, i.e. $\Delta\epsilon = 0$, $\Delta\varphi \sim \mathcal{U}[0; 2\pi)$, $P = Z = 1$.

For reference, we also show the results for a single equal-power interferer if that interferer is assumed to be Gaussian. We determine the iterative decoding threshold of our ad-hoc protograph ensemble for these interference models by applying (quantized) density evolution, making the use of equations (4) and (5). Since the interferer power is fixed, we define the iterative decoding threshold as the largest noise power per dimension σ_n^2 such that error-free transmission is possible. Figure 7 shows the density evolution threshold of ad-hoc protograph ensemble compared to the channel capacity in each of the three interferer models.

As shown in Figure 7, the QPSK interferer with random phase gives the best threshold, whereas the Gaussian interferer gives the worst threshold. We can explain this by using Figure 4. In the absence of noise, the received signal, $y(t)$ is on a circle around the transmitted signal, $x(t)$. To depict $y(t)$, we can simply draw four circles around the four QPSK constellation points. It can be observed that these circles intersect. However, the probability to pick exactly the intersection point goes to zero. Thus, we can reach a mutual information of two for the QPSK interferer with random phase. For the phase aligned QPSK interferer, the mutual information between $y(t)$ and $x(t)$ reaches one in the absence of noise. Thus for the interfered part we can get a rate of at most one. Hence the phase aligned QPSK interferer gives a lower threshold than the QPSK interferer with random phase. For the Gaussian interferer case, the mutual information is limited by the QPSK capacity at $E_s/N_0 = 0$ dB, where the mutual information at 0 dB is 0.96 for the interfered part. Thus the Gaussian interference model show the worst threshold compared to phase aligned QPSK interferer and QPSK intererfer with random phase.

IV. NUMERICAL RESULTS

For the numerical results we drop the simplified surrogate channel model and focus on two more realistic RA channels. The first set of numerical results makes use of a physical

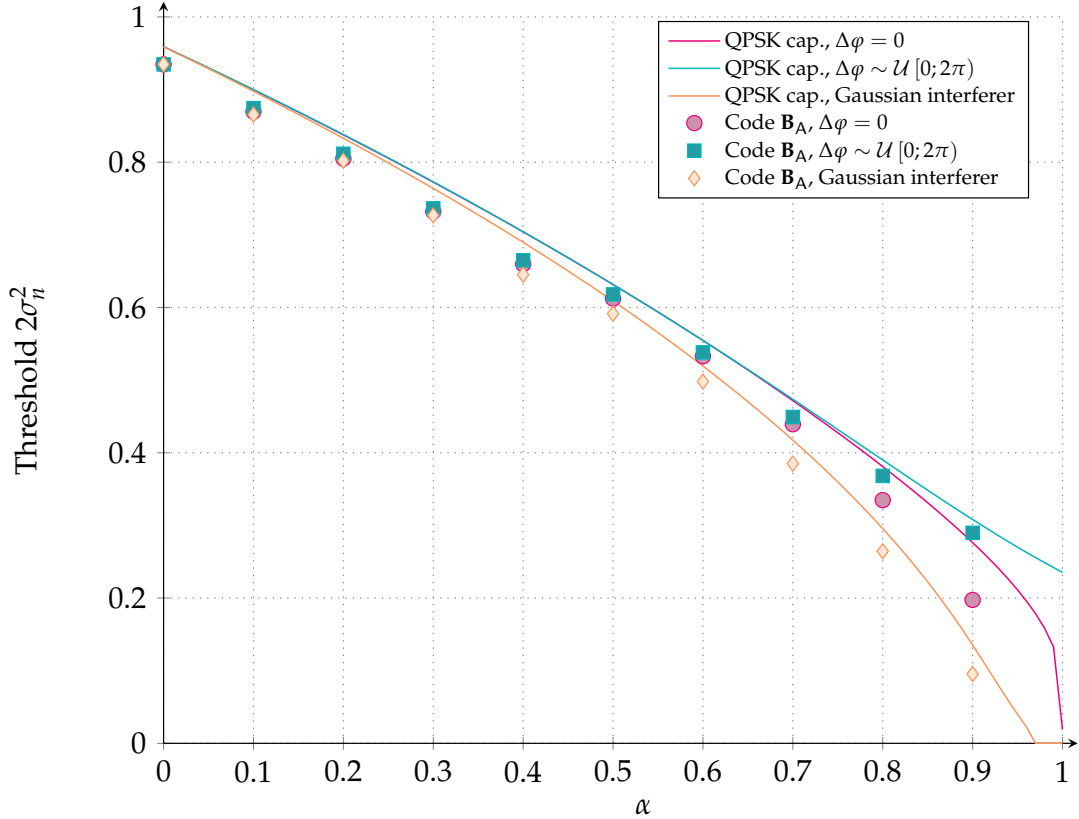


Fig. 7: Noise threshold for the code ensemble described by the base matrix \mathbf{B}_A , calculated using quantized density evolution, compared to capacity, on a QPSK channel with a single equal power interferer as the interferer overlap, α , is varied. Three different models for the interferer are considered, a time and phase aligned QPSK signal, a time aligned and random phase QPSK signal and a Gaussian interferer.

layer abstraction where the interference is Gaussian, but not necessarily constant over the αn_s symbols of a modulated codeword. In the second set of numerical results the complete physical layer is implemented and hence the Gaussian assumption on the interference is dropped. While the abstracted physical layer model is a common approach to get first-level insights in the system performance [27], (long) physical layer simulations serve as a confirmation of the results. If the identified trends are still present, physical layer results may give evidence on the validity of the surrogate channel model adopted for the code design.

The assumptions common to both set of numerical results are summarized in the following. Users transmit $d = 2$ replicas according to the asynchronous RA protocol described in Section II-A. Replicas are affected by multiple access interference and by AWGN noise, with $E_s/N_0 = 6$ dB. All replicas are received with the same normalized power $P = 1$, thanks

to perfect power control. For simplicity, we normalize all duration to the packet length t_p . The VF duration is set to $200 t_p$, while the receiver decoding window is $W = 600 t_p$. The receiver decoding window shift is set to $\Delta W = 20 t_p$.

The performance metric we use to compare the performance of different error correcting codes in the asynchronous random access setting is the PLR p_l , as a function of the channel load G . The PLR is the average probability that a user cannot be correctly recovered at the receiver, at the end of the SIC process.

A. Abstracted Physical Layer

To abstract the physical layer, we make use of so-called decoding regions [44]. Based on a certain interference pattern, we decide whether the decoding of a replica is successful or not, simply by checking whether the corresponding noise plus interference vector falls within the decoding region. An m -dimensional decoding region can be seen as an extension of a threshold model to channels with m -dimensional channel parameters, such as block fading channels.

1) *Decoding Region for Random Code Ensembles:* We assume that replicas are received with interference whose power may vary over the replica symbols. We resort to a *block interference channel* [41], where a replica experiences various blocks of constant interference. Recall that the interference is assumed to be drawn from a complex white Gaussian process $\mathcal{CN}(0, 2\sigma_t^2)$, with $2\sigma_t^2$ being the interference power (see also Section III-C1).

Let us call m' the maximum number of interferers affecting a replica. Let us denote by m , $1 \leq m \leq m' + 1$, the number of *different* interference plus noise levels that are present over the considered replica. Define

$$\boldsymbol{\sigma}^{(2)} = \left[\underbrace{\sigma_n^2 + \frac{1}{2}}_{\sigma_1^2}, \dots, \underbrace{\sigma_n^2 + \frac{m}{2}}_{\sigma_m^2} \right] \quad (9)$$

as the ordered interference plus noise vector which contains the m different noise plus interference levels in the replica. Let $\boldsymbol{\alpha} = [\alpha_1, \dots, \alpha_m]$, where α_j , $j \in \{1, \dots, m\}$, is the fraction of a replica subject to the interference plus noise of power $(\sigma_n^2 + \frac{j}{2})$ per dimension. Clearly, $\sum_{j=1}^m \alpha_j \leq 1$ and $\alpha_j \in (0, 1]$. Recalling that $C(\sigma^2)$ is the QPSK constraint AWGN channel capacity for a given σ^2 , the outage capacity C_o under the Gaussian interference assumption is

$$C_o(\boldsymbol{\alpha}, \sigma_n^2, \boldsymbol{\sigma}^{(2)}) = \left(1 - \sum_{j=1}^m \alpha_j \right) C\left(\frac{1}{2\sigma_n^2}\right) + \alpha_1 C\left(\frac{1}{2\sigma_1^2}\right) + \dots + \alpha_m C\left(\frac{1}{2\sigma_m^2}\right).$$

For a fixed transmission rate R , we define the decoding region \mathcal{D} [33], [44] as

$$\mathcal{D} = \left\{ \boldsymbol{\sigma}^{(2)} \in \mathbb{R}_+^m, \boldsymbol{\alpha} \in (0, 1]^m \mid \sum_{j=1}^m \alpha_j \leq 1 \wedge R < C_o(\boldsymbol{\sigma}^{(2)}, \sigma_n^2, \boldsymbol{\alpha}) \right\}. \quad (10)$$

Every m' -user collision resulting in $(\boldsymbol{\alpha}, \sigma_n^2, \boldsymbol{\sigma}^{(2)}) \in \mathcal{D}$ can be resolved.

A possibility to numerically evaluate the performance of a random code ensemble which achieves a fraction β of the outage capacity with $\beta < 1$, is to compute the decoding region $\mathcal{D}' \subset \mathcal{D}$ as

$$\mathcal{D}' = \left\{ \boldsymbol{\sigma}^{(2)} \in \mathbb{R}_+^m, \boldsymbol{\alpha} \in (0, 1]^m \mid \sum_{j=1}^m \alpha_j \leq 1 \wedge R < \beta C_o(\boldsymbol{\sigma}^{(2)}, \sigma_n^2, \boldsymbol{\alpha}) \right\}.$$

For the abstracted physical layer simulations we follow the steps from the literature [44]. We generate realizations of packet collisions for a certain channel load G . For each of the n_s codeword symbols of a replica, we compute an instantaneous noise plus interference power. We assume that for each codeword symbol we have knowledge of the number of interferers due to ideal detection. Thus, we group the n_s instantaneous noise plus interference power values into m blocks, sort them according to the number of interferers, average over the noise plus interference power in every block to finally obtain the ordered interference plus noise vector $\boldsymbol{\sigma}^{(2)}$ in (9). Successful decoding is declared if $(\boldsymbol{\alpha}, \sigma_n^2, \boldsymbol{\sigma}^{(2)}) \in \mathcal{D}$ (or $\in \mathcal{D}'$).

2) *Decoding Region for LDPC Code Ensembles:* For LDPC protograph ensembles the decoding region is computed slightly differently from (10). Since for structured code ensembles not only the power and fraction, but also the position of the interferer is important, we introduce a length- n_b protograph noise plus interference vector $\boldsymbol{\sigma}_p^{(2)} = [(\sigma_n^2 + \sigma_l^2)_0, \dots, (\sigma_n^2 + \sigma_l^2)_{n_b-1}]$. An element $(\sigma_n^2 + \sigma_l^2)_j$ corresponds to the specific signal plus interference level for a VN of type j . Then, the decoding region in (10) can be restated as

$$\mathcal{D}'' = \left\{ \boldsymbol{\sigma}_p^{(2)} \in \mathbb{R}_+^{n_b} \mid I_{\text{APP}}(j) \rightarrow 1 \forall j \in \{0, \dots, n_b - 1\} \right\}.$$

The signal plus interference level $(\sigma_n^2 + \sigma_l^2)_j$ for a VN of type j is determined as follows. For a certain channel load G , realizations of packet collisions are generated. For each of them one may determine an instantaneous bit-wise noise plus interference power for each of the n codeword bits. Then, for each of the $n_b - p_b$ unpunctured VN types in the protograph we determine an average noise plus interference level by averaging over $n/(n_b - p_b)$ subsequent values of the instantaneous bit-wise noise plus interference powers yielding $\boldsymbol{\sigma}_p^{(2)}$. Decoding is successful only if $\boldsymbol{\sigma}_p^{(2)} \in \mathcal{D}''$.

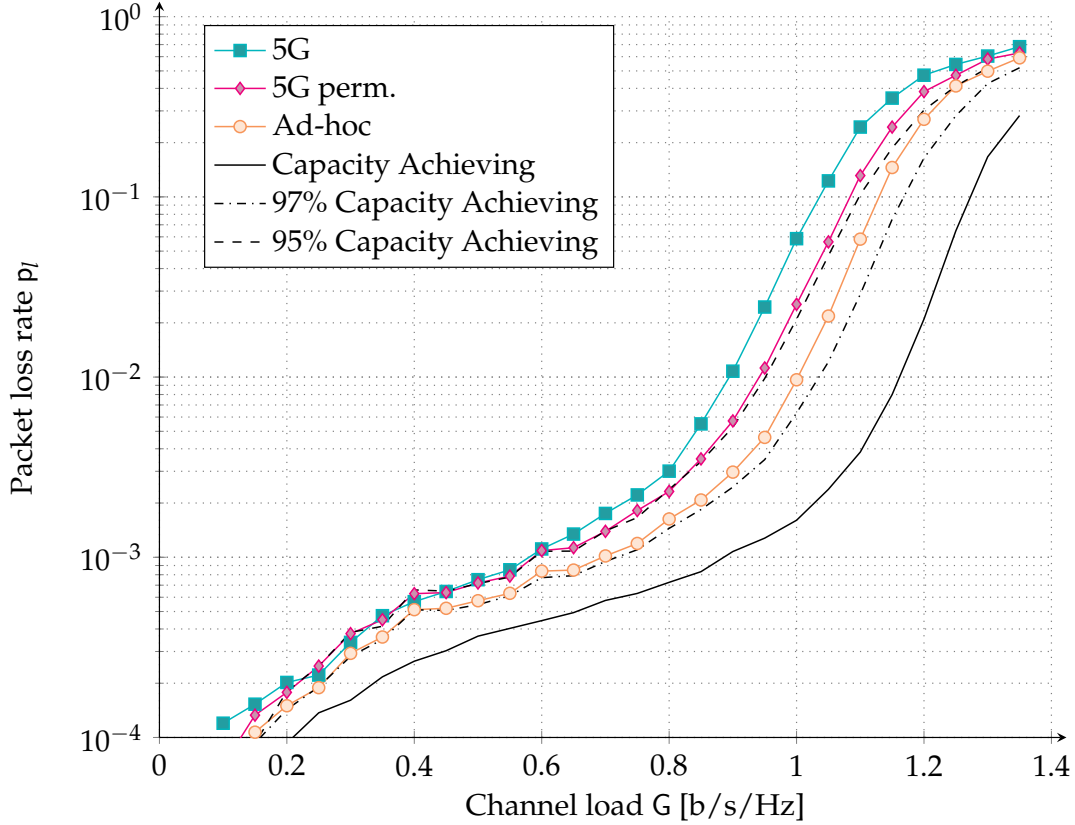


Fig. 8: PLR vs. channel load G for the 5G, permuted 5G, and ad-hoc LDPC protograph code ensembles for asynchronous RA setting with abstracted physical layer. The 5G corresponds to the ensemble with base matrix \mathbf{B}_{5G} . The 5G perm. corresponds to the ensemble with base matrix \mathbf{B}_{5G}^π . Ad-hoc corresponds to the ensemble with base matrix \mathbf{B}_A .

3) *Simulation Results:* The PLR performance assuming the three different protograph code ensembles from Section III-D is shown in Figure 8. For reference, the performance for a capacity achieving code ensemble, one which achieves 97% of capacity and one which achieves 95% of capacity are also shown (solid black, dot-dashed black and dashed black curves, respectively). In the entire channel load range, the ad-hoc design (base matrix \mathbf{B}_A) visibly outperforms both 5G-based solutions (base matrices \mathbf{B}_{5G} and \mathbf{B}_{5G}^π). The simple yet insightful observation that the beginning and the end of a packet shall be strongly protected by the channel code, leads to a beneficial performance gain also when the overall multiple access interference comes into play. In particular, for a target PLR of 10^{-3} , the channel load supported can be extended from 0.6 [b/s/Hz] of the 5G-based solutions to 0.7 [b/s/Hz] of the ad-hoc LDPC design, resulting in a 0.1 [b/s/Hz] or 17% gain. Similarly, at PLR of 10^{-2} , the channel load supported can be extended from 0.9 [b/s/Hz] of the 5G-based solutions to

1.0 [b/s/Hz] of the ad-hoc LDPC design, resulting in a 0.1 [b/s/Hz] or 11% gain. For a fixed channel load operating point, the gain is even more remarkable.

Finally, observe that there is still a visible gap to capacity achieving code ensembles. One may erroneously conclude that the constant interfering power assumption of the surrogate channel model in Section III-C is inaccurate, yielding a design that is penalized on the Gaussian interference channel with varying interference powers. However, we found that even a small loss in error correction performance may have a big effect on the PLR. To underpin this observation, consider a code ensemble that achieves 95% of the outage capacity. Observe that this code ensemble performs similarly to the permuted 5G-like design and worse than our ad-hoc design for the surrogate channel. A possible reason for the drastic impact of the code performance on the asynchronous random access PLR might due to the SIC: in case a replica cannot be correctly decoded due to the sub-optimality of the error correcting code, it may arrest the SIC process and cause multiple packet losses. Consider a code ensemble that achieves 97% of the outage capacity instead of 95%. Observe from the figure that such a minor improvement on the code design can result in gains of up to 0.1 [b/s/Hz].

In order to confirm the trends identified with the abstracted physical layer and to overcome its inherent limitations, in the following Section we will resort to simulate the physical layer performance of the proposed LDPC codes.

B. Finite-Length Physical Layer Simulations with the Designed LDPC Codes

We consider here a (960, 480) LDPC codes obtained from the base matrices in Section III-D. The code parameters are chosen to fit in the context of short packet communications.⁷ Each users selects a codeword uniformly at random from the codebook. The codeword is QPSK modulated, and two instances (replicas) are transmitted. Each of the modulated replicas are sent over the asynchronous RA channel undergoing the protocol rules as described in Section II. Ideal channel estimation is assumed, so that the receiver can perfectly compensate for the phase offset. After channel estimation, soft-LLR values are computed based on the perfect interference power knowledge. Note that the interference contribution here is the superposition of possibly multiple QPSK modulated, equal-power signals, with random phase offsets, corresponding to all replicas that are concurrently received. It is important to stress that this assumption departs from the Gaussian interference

⁷Packets in the order of hundreds of information bits are typical of M2M applications. An example is the early data transmission procedure available in release 15 of 3GPP, where terminals are allowed to piggyback data on message 3 of the PRACH with sizes between 328 and 1000 information bits [2].

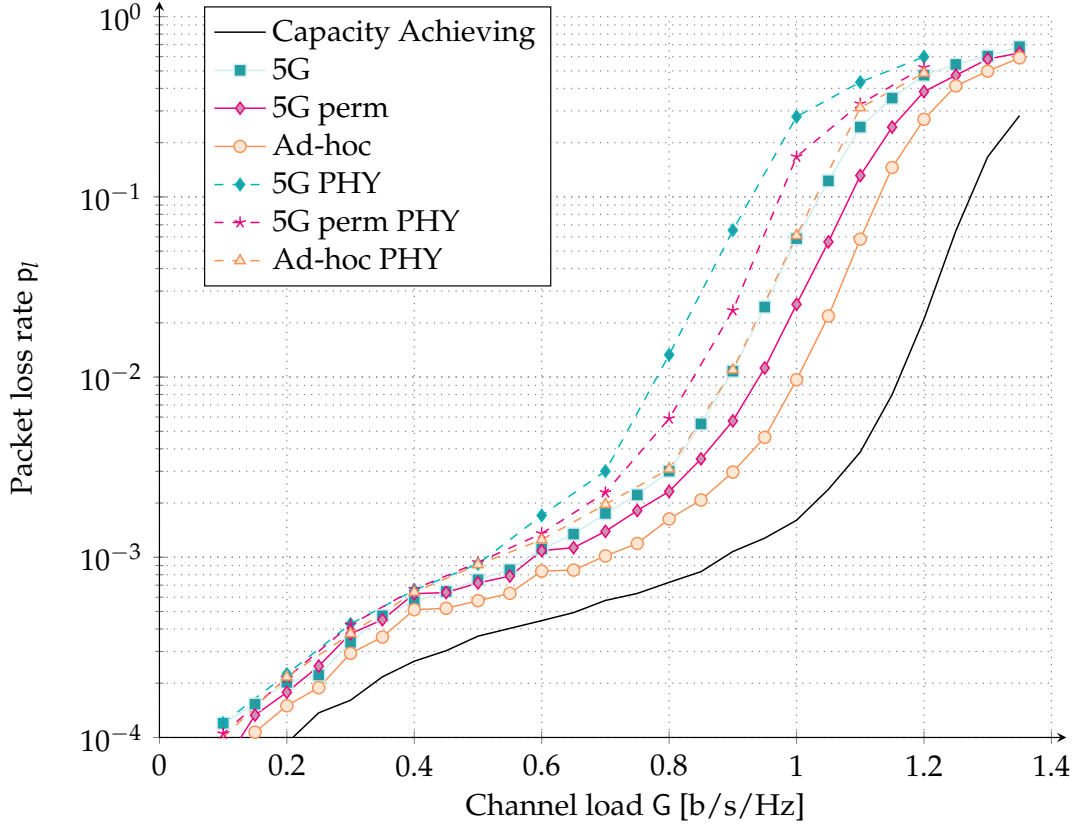


Fig. 9: Dashed: PLR vs. channel load G for the asynchronous RA protocol with replicas protected by different $(960, 480)$ LDPC codes, as a result of physical layer simulations. Solid: curves from Figure 8 assuming abstracted physical layer. The 5G corresponds to the ensemble with base matrix \mathbf{B}_{5G} . The 5G perm. corresponds to the ensemble with base matrix \mathbf{B}_{5G}^π . Ad-hoc corresponds to the ensemble with base matrix \mathbf{B}_A .

assumption, especially when the number of interfering replicas is small. A standard belief propagation LDPC decoder with a maximum of 50 decoding iterations is used to counteract the effect of noise and multiple access interference. If the decoder is successful, the replica is removed from the received signal together with its twin, so that no residual interference power is left after cancellation.

The dashed curves in Figure 9 show the PLR performance versus channel load of the asynchronous RA scheme with replicas protected with a code described by the base matrix \mathbf{B}_A (named Ad-hoc PHY), \mathbf{B}_{5G}^π (named 5G perm PHY), or \mathbf{B}_{5G} (named 5G PHY) respectively. The solid curves are resumed from Figure 8 and depict results for the abstracted physical layer. Observe that the relative gap between the ad-hoc LDPC design, permuted 5G design, as well as the 5G design is preserved, since all three codes suffer from a similar degradation

due to finite length effects. For the ad-hoc design, at a target PLR of 10^{-3} , the supported channel load is reduced from 0.7 [b/s/Hz] to ~ 0.6 [b/s/Hz]. Similarly at 10^{-2} the achieved channel load becomes 0.9 [b/s/Hz] compared to 1 [b/s/Hz] when the abstract physical layer is considered. In line with the ad-hoc design, also the 5G code suffers from a degradation of ~ 0.1 [b/s/Hz] in the channel load region of interest.

Interestingly, although the ad-hoc LDPC code is designed for a surrogate channel, both the abstract physical layer and the full physical layer simulations confirm the beneficial impact on the asynchronous random access protocol. The abstract physical layer model is able to hinge the performance tendencies that are subject to a penalty when one considers the precise physical layer. Such penalty mostly originates from finite-length effects of the channel code. The assumption of Gaussianity for the multiple access interference, as well as constant interfering power appears to be reasonable and thus can be exploited to simplify the channel code design.

V. CONCLUSIONS

This work presents protograph LDPC code designs for asynchronous RA with SIC. For the code design we make use of a simplified surrogate channel model which assumes Gaussian interference and constant interfering power over the interfered part of a packet. Considering more realistic RA channels, we show that the proposed designs for the surrogate channel perform close to theoretical limits. Gains of 17%, in supported channel load at a packet loss rate of 10^{-2} are observed w.r.t. an off-the-shelf code. In contrast to literature where the physical layer code performance is often abstracted by means of decoding thresholds or decoding regions, physical layer LDPC code simulations for short blocks are performed, yielding a more realistic estimate of the achievable supported channel load (for a fixed target packet error rate). We find that abstracting the physical layer overestimates the performance for our setup by approximately 10% in supported channel load, at a packet loss rate of 10^{-2} .

ACKNOWLEDGMENTS

The authors would like to thank Nina Grosheva for her support in the design of the asynchronous medium access simulation environment during its early stages.

REFERENCES

- [1] A. Osseiran, F. Boccardi, V. Braun, K. Kusume, P. Marsch, M. Maternia, O. Queseth, M. Schellmann, H. Schotten, H. Taoka, H. Tullberg, M. A. Uusitalo, B. Timus, and M. Fallgren, "Scenario for 5G mobile and wireless communications: the vision of the METIS project," *IEEE Commun. Mag.*, vol. 52, no. 5, pp. 26–35, may 2014.

- [2] 3GPP, “TR 21.915 v1.1.0, Release 15 Description,” 2019.
- [3] A. Laya, L. Alonso, and J. Alonso-Zarate, “Is the Random Access Channel of LTE and LTE-A Suitable for M2M Communications? A Survey of Alternatives,” *IEEE Commun. Surveys Tuts.*, vol. 16, no. 1, pp. 4–16, First Quarter 2014.
- [4] N. Abramson, “The ALOHA system: Another alternative for computer communications,” in *Proc. Fall Joint Computer Conf. (AFIPS)*, vol. 37, Montvale, N. J., nov 1970, pp. 281–285.
- [5] L. G. Roberts, “ALOHA packet system with and without slots and capture,” *Proc. SIGCOMM Computer Commun. Review*, vol. 5, no. 2, pp. 28–42, apr 1975.
- [6] E. Casini, R. De Gaudenzi, and O. Del Rio Herrero, “Contention resolution diversity slotted ALOHA (CRDSA): An enhanced random access scheme for satellite access packet networks,” *IEEE Trans. Wireless Commun.*, vol. 6, no. 4, 2007.
- [7] G. Liva, “Graph-Based Analysis and Optimization of Contention Resolution Diversity Slotted ALOHA,” *IEEE Trans. Commun.*, vol. 59, no. 2, pp. 477–487, feb 2011.
- [8] E. Paolini, G. Liva, and M. Chiani, “Coded Slotted ALOHA: A Graph-Based Method for Uncoordinated Multiple Access,” *IEEE Trans. Inf. Theory*, vol. 61, no. 12, pp. 6815–6832, oct 2015.
- [9] E. Sandgren, A. Graell i Amat, and F. Brännström, “On Frame Asynchronous Coded Slotted ALOHA: Asymptotic, Finite Length, and Delay Analysis,” *IEEE Trans. Commun.*, vol. 65, no. 2, pp. 691–703, feb 2017.
- [10] C. Stefanovic and P. Popovski, “ALOHA Random Access that Operates as a Rateless Code,” *IEEE Trans. Commun.*, vol. 61, no. 11, pp. 4653–4662, nov 2013.
- [11] Y. Yu and G. B. Giannakis, “High-Throughput Random Access Using Successive Interference Cancellation in a Tree Algorithm,” *IEEE Trans. Inf. Theory*, vol. 53, no. 12, pp. 4628–4639, dec 2007.
- [12] J. L. Massey, “Collision-Resolution Algorithm and Random-Access Communication,” *Multi-User Communication Systems*, vol. Editor G. Longo, pp. 73–137, 1981.
- [13] R. Gallager, “A perspective on Multiaccess Channels,” *IEEE Trans. Inf. Theory*, vol. 31, no. 2, pp. 124–142, mar 1985.
- [14] M. Luby, M. Mitzenmacher, A. Shokrollahi, and D. A. Spielman, “Improved Low-Density Parity-Check Codes Using Irregular Graphs,” *IEEE Trans. Inf. Theory*, vol. 47, no. 2, pp. 585–598, feb 2001.
- [15] T. J. Richardson, A. Shokrollahi, and R. L. Urbanke, “Design of Capacity-Approaching Irregular Low-Density Parity-Check Codes,” *IEEE Trans. Inf. Theory*, vol. 47, no. 2, pp. 619–637, feb 2001.
- [16] M. Ivanov, F. Brännström, A. Graell i Amat, and P. Popovski, “Error Floor Analysis of Coded Slotted ALOHA Over Packet Erasure Channels,” *IEEE Commun. Lett.*, vol. 19, no. 3, pp. 419–422, mar 2015.
- [17] A. Graell i Amat and G. Liva, “Finite-length analysis of irregular repetition slotted aloha in the waterfall region,” *IEEE Communications Letters*, vol. 22, no. 5, pp. 886–889, 2018.
- [18] K. R. Narayanan and H. D. Pfister, “Iterative Collision Resolution for Slotted ALOHA: An Optimal Uncoordinated Transmission Policy,” in *Proc. 7th Int. Symp. on Turbo Codes and Iterative Information Processing (ISTC)*, Gothenburg, Sweden, aug 2012, pp. 136–139.
- [19] Y. Polyanskiy, “A Perspeticve on Massive Random-Access,” in *Proc. IEEE Intl. Symp. Information Theory (ISIT)*, Aachen, Germany, jun 2017, pp. 2523–2527.
- [20] M. Effros, V. Kostina, and R. C. Yavas, “Random Access Channel Coding in the Finite Blocklength Regime,” in *Proc. IEEE Intl. Symp. Information Theory (ISIT)*, Vail, CO, USA, jun 2018.
- [21] O. Ordentlich and Y. Polyanskiy, “Low Complexity Scheme for the Random Access Gaussian Channel,” in *Proc. IEEE Intl. Symp. Information Theory (ISIT)*, Aachen, Germany, jun 2017, pp. 2528–2532.
- [22] A. Vem, K. R. Narayanan, J. Cheng, and J.-F. Chamberland, “A User-Independent Serial Interference Cancellation

- Based Coding Scheme for the Unsourced Random Access Gaussian Channel,” in *Proc. IEEE Inf. Theory Work. (ITW)*, Kaohsiung, Taiwan, nov 2017, pp. 121–125.
- [23] R. Calderbank and A. Thompson, “CHIRRUP: a Practical Algorithm for Unsourced Multiple Access,” *Available on arxiv.org*, 2018.
- [24] V. K. Amalladinne, J.-F. Chamberland, and K. R. Narayanan, “A Coded Compressed Sensing Scheme for Uncoordinated Multiple Access,” *Available on arxiv.org*, 2018.
- [25] C. Kissling, “Performance Enhancements for Asynchronous Random Access Protocols over Satellite,” in *Proc. IEEE Int. Conf. on Commun. (ICC)*, Kyoto, Japan, jun 2011, pp. 1–6.
- [26] R. De Gaudenzi, O. del Rio Herrero, G. Acar, and E. G. Barrabes, “Asynchronous Contention Resolution Diversity ALOHA: Making CRDSA Truly Asynchronous,” *IEEE Trans. Wireless Commun.*, vol. 13, no. 11, pp. 6193–6206, nov 2014.
- [27] F. Clazzer, C. Kissling, and M. Marchese, “Enhancing Contention Resolution ALOHA using Combining Techniques,” *IEEE Trans. Commun.*, vol. 66, no. 6, pp. 2576–2587, jun 2018.
- [28] T. Akyildiz, U. Demirhan, and T. M. Duman, “Asymptotic analysis of contention resolution ALOHA with replica concatenation,” in *2019 IEEE International Conference on Communications (ICC)*, Shanghai, China, May 2019, pp. 1–6.
- [29] C. Kissling and F. Clazzer, “LDPC code performance and optimum code rate for contention resolution diversity ALOHA,” in *IEEE Global Communications Conference (GLOBECOM)*, Atlanta, GA, USA, Dec 2013, pp. 2932–2938.
- [30] B. Matuz, F. Clazzer, S. J. Johnson, S. Jayasooriya, and M. Shirvanimoghaddam, “LDPC code design for asynchronous random access,” in *2018 IEEE 10th International Symposium on Turbo Codes Iterative Information Processing (ISTC)*, Hong Kong, Dec 2018, pp. 1–5.
- [31] B. Masnick and J. Wolf, “On linear unequal error protection codes,” *IEEE Trans. Inf. Theory*, vol. 13, no. 4, pp. 600–607, oct 1967.
- [32] G. Caire and E. Biglieri, “Parallel Concatenated Codes with Unequal Error Protection,” *IEEE Trans. Commun.*, vol. 46, no. 5, pp. 565–567, may 1998.
- [33] J. J. Boutros, A. Guillen i Fabregas, and E. Calvanese, “Analysis of Coding on Non-Ergodic Block fading Channels,” in *Proc. 2005 Allerton Conf. on Communication, Control and Computing*, 2005.
- [34] J. J. Boutros, A. Guillen i Fabregas, E. Biglieri, and G. Zemor, “Low-Density Parity-Check Codes for Nonergodic Block-Fading Channels,” *IEEE Trans. Inf. Theory*, vol. 56, no. 9, pp. 4286–4300, sep 2010.
- [35] M. Chiani, “Noncoherent Frame Synchronization,” *IEEE Trans. Commun.*, vol. 58, no. 5, pp. 1536–1545, may 2010.
- [36] F. Clazzer, F. Lázaro, G. Liva, and M. Marchese, “Detection and Combining Techniques for Asynchronous Random Access with Time Diversity,” in *Proc. 11th Int. ITG Conf. on Systems, Commun. and Coding (SCC)*, Hamburg, Germany, feb 2017, pp. 1–6.
- [37] U. Mengali and A. N. D’Andrea, *Synchronization Techniques for Digital Receivers*. Springer Science+Business Media, 1997.
- [38] J. Thorpe, “Low-density parity-check (LDPC) codes constructed from protographs,” NASA JPL, Pasadena, CA, USA, IPN Progress Report 42-154, aug 2003.
- [39] H. Uchikawa, “Design of Non-Precoded Protograph-Based LDPC Codes,” in *IEEE International Symposium on Information Theory*, Honolulu, HI, USA, jun 2014, pp. 2779–2783.
- [40] G. Liva and M. Chiani, “Protograph LDPC Codes Design Based on EXIT Analysis,” in *Proc. IEEE Global Commun. Conf. (GLOBECOM)*, nov 2007, pp. 3250–3254.
- [41] R. J. McEliece and W. E. Stark, “Channels with Block Interference,” *IEEE Trans. Inf. Theory*, vol. IT-30, no. 1, pp. 44–53, jan 1984.

- [42] T. Y. Chen, D. Divsalar, J. Wang, and R. D. Wesel, "Protograph-based Raptor-like LDPC codes for rate compatibility with short blocklengths," in *Proc. IEEE Global Commun. Conf. (GLOBECOM)*, Houston, TX, USA, dec 2011, pp. 1–6.
- [43] Huawei and HiSilicon, "R1-1706970 LDPC design for eMBB data," 2017, RAN1 #89.
- [44] P. Pulini, G. Liva, and M. Chiani, "Unequal Diversity LDPC Codes for Relay Channels," *IEEE Trans. Wireless Commun.*, vol. 12, no. 11, pp. 5646–5655, nov 2013.